

# Structural Change of Myosin Motor Domain and Nucleotide Dissociation

Fumiko Takagi<sup>\*†‡</sup>, and Macoto Kikuchi<sup>†‡</sup>

<sup>†</sup>Formation of Soft Nanomachines, Core Research for Evolutional Science and Technology, Japan Science and Technology Agency, Yamadaoka, Suita, Osaka 565-0871, Japan, and <sup>‡</sup>Cybermedia Center Osaka University, Toyonaka, Osaka 560-0043, Japan

Submitted to Proceedings of the National Academy of Sciences of the United States of America

**We investigated the structural relaxation of myosin motor domain from the pre-power stroke state to the near-rigor state using molecular dynamics simulation of a coarse-grained protein model. To describe the structural change, we propose a “dual Gō-model,” a variant of the Gō-like model that has two reference structures. The nucleotide dissociation process is also studied by introducing a coarse-grained nucleotide in the simulation. We found that the myosin structural relaxation toward the near-rigor conformation cannot be completed before the nucleotide dissociation. Moreover, the relaxation and the dissociation occurred cooperatively when the nucleotide was tightly bound to the myosin head. The result suggested that the primary role of the nucleotide is to suppress the structural relaxation.**

molecular dynamics simulation — dual-Gō model — coarse-grained protein — coarse-grained nucleotide — strain sensor

## Introduction

The mechanism of biomolecular motors is one of the major topics in biophysics. Among a number of such systems that have been found so far, the actomyosin motor is of a particular interest, because it is responsible for muscle contraction and cellular movements in eukaryotic cells. Myosin moves unidirectionally along the actin filament using chemical energy released by ATP hydrolysis [1, 2, 3]. It is widely recognized that the efficiency of this energy conversion is very high compared with macroscopic artificial machines, in spite of the fact that biomolecular motors work under a noisy environment in the cell. In fact, the free energy released during each ATP hydrolysis is only about  $20k_B T$ ; therefore the thermal fluctuation should be appreciable. Although recent progress in imaging and of nanomanipulation has enabled the observation of single molecules, the movement mechanism of the actomyosin motor is still not understood.

There has been a long-standing controversy between the tight-coupling (lever-arm) model and the loose-coupling model. X-ray crystallographic studies have revealed that the angle of the neck domain changes relative to the motor domain, depending on the nucleotide state. The “lever-arm” model was proposed based on these observations, in which the structural change of myosin is tightly coupled with the ATP hydrolysis cycle, and directly causing a stepwise sliding motion. It was shown, however, that the sliding distance of the myosin along the actin filament per ATP at the muscle contraction can be much longer than the displacement predicted by the lever-arm-like structural change of a single myosin molecule [4]. Moreover, it is questionable whether a material as soft as proteins can accurately switch its conformation in the same way as a macroscopic machine under thermal

fluctuation.

In the “loose-coupling” model, in contrast, the structural change does not always correspond to a step in a one-to-one correspondence; the motion is intrinsically stochastic and thermal fluctuation is an essential ingredient for its mechanism [5]. The simplest class of models that produce the loose-coupling mechanism is based on a thermal ratchet, in which a myosin molecule is treated as a Brownian particle that moves along a periodic and asymmetric potential under both thermal noise and non-thermal perturbations [6, 7]. Although ratchet systems can, in fact, exhibit unidirectional flow in a noisy environment, a high efficiency comparable to that of the actomyosin system is found difficult to achieve using only a simple ratchet system. Even if the ratchet models do to express some essence of the mechanism of the biomolecular motor, they are too much simplified and we should say that the connection with the real actomyosin system is rather vague. In particular, since the myosin is expressed as a particle, the effect of its conformational change is, at best, only implicitly taken into account. A somewhat more realistic modelling is desirable, which can reflect the chain conformation.

Recently, it was revealed by single molecule experiments that the chemomechanical cycle of the myosin head is controlled by a load on the actomyosin crossbridge [8, 9, 10]. The observation suggested that the rate of ADP release from the myosin head depends on the force acting on myosin; namely, the chemical reaction rate varies with the deformation of the myosin. If the myosin head indeed acts as such a “strain sensor,” this would be reminiscent of a classical model by A. Huxley [11]; in this model, the myosin head is supposed to undergo Brownian motion and change into a tightly bound state to the actin filament triggered by a structure dependent chemical reaction.

The relationship between structure and function of proteins has long been investigated. Thus far, mainly the static aspects of proteins have been considered, for example, the classical “lock and key” model of an enzyme. Recently, the role of structural fluctuations, or that of a more drastic structural change, including “partial unfolding,” on protein functions has become a subject of growing interest. Although there have been many experimental studies to clarify the dynamical processes of protein at a functional level, it is still difficult to observe the structural changes with high resolution in

Conflict of interest footnote placeholder

Insert 'This paper was submitted directly to the PNAS office.' when applicable.

\* To whom correspondence should be addressed. E-mail: fumiko@cp.cmc.osaka-u.ac.jp

©2006 by The National Academy of Sciences of the USA

both space and time. Computer simulations serve as possible alternatives. Typical computational studies treated equilibrium fluctuations near a crystal structure using the all-atom model [12, 13] or the elastic network model [14]; although these types of simulations cannot deal with large-scale structural change, the low-frequency fluctuation modes were found to be consistent with the direction of motion of the structural change associated with the function.

Some attempts have been made to simulate a larger structural change beyond the elastic regime using a class of models called the  $G\bar{o}$ -like model [15]. According to the recently developed theory of spontaneous protein folding, the protein energy landscape has a funnel-like global shape toward the native structure. The  $G\bar{o}$ -like model is certainly the simplest class of models that can realize a funnel-like landscape [16, 17] and has successfully described the folding process of small proteins. It is, however, not suitable for the study of a change between two conformations, because only the interaction between the pairs of residues that contact each other in the native state are taken into account; the conformation other than the native state becomes too unstable as a result. Thus, a model is desirable in which two conformations can be embedded. Here, we introduce a new model bearing this property as a variant of the  $G\bar{o}$ -like model.

In this paper, we investigate the dynamics of the myosin conformational change from the pre-power stroke state to the near-rigor state by molecular dynamics simulations of a coarse-grained protein. This process is called “power stroke” because the angle of the lever-arm changes remarkably, and it is considered in the lever-arm model that this structural change directly causes the force generation. To describe the structural change, we propose the “dual  $G\bar{o}$ -model.” The dissociation process of the nucleotide that accompanies the conformational change is also involved in the simulation by introducing a coarse-grained nucleotide. To our knowledge, the ligand at the binding site has not been considered explicitly in coarse-grained protein simulations, possibly because the primary role of ATP is considered to be the release of chemical energy through hydrolysis, and the excluded volume effect of the molecule has not been investigated. We, however, consider that the presence or absence of nucleotides in the binding site would profoundly affect the structural fluctuation of the protein. Therefore, it is important to perform simulations including the nucleotide.

## Results

First, we introduce the dual  $G\bar{o}$ -model. While only the native structure is taken as a reference structure for the potential energy function in the standard  $G\bar{o}$ -like models, the dual  $G\bar{o}$ -like model takes two reference structures, structure 1 and structure 2, in the effective potential. For the interaction between “native-contact” pairs, each potential energy function has two minima corresponding to two reference structures. To study the relaxation process from structure 2 to structure 1, the minimum corresponding to structure 2 is given a slightly higher energy than that of structure 1 to make structure 1 more stable. In this study, we used a model based on one of the  $C_\alpha$   $G\bar{o}$ -like models [18, 19], which involves local interactions such as bond length, bond angle, and dihedral angle interactions as well as the native-contact interaction. For these local

interactions, we set that each potential energy function has two minima of the same depth corresponding to two reference structures.

As reference structures, we choose X-ray crystallography structures of *Dictyostelium discoideum* myosin II: the near-rigor structure without nucleotide, 1Q5G [20] for structure 1 and the pre-power stroke structure with ADP- $P_i$  analog, 1VOM [21] for structure 2 (Fig. 1). The initial structure is the pre-power stroke structure with a coarse-grained nucleotide (Fig. 2) located at the nucleotide-binding site.

Typical time courses of the distance root mean square deviation (dRMSD) are shown in Fig. 3 for (a)  $k_{p-n} = 0.6$  and (b) 0.7, where  $k_{p-n}$  is the strength parameter of the protein-nucleotide interaction. The dRMSD from the near-rigor structure is defined as

$$\text{dRMSD} = \sqrt{\frac{2}{N(N-1)} \sum_{i < j} (r_{ij} - r_{ij}^{(1)})^2}, \quad [1]$$

in which  $r_{ij} = |\mathbf{r}_{ij}| = |\mathbf{r}_i - \mathbf{r}_j|$  is the distance between  $C_\alpha$  carbons of the  $i$ th and  $j$ th residues in the given conformation, and  $r_{ij}^{(1)}$  indicates their distance in the near-rigor structure. At the initial conformation, the dRMSD of  $\sim 3.9\text{\AA}$ , and decreases rapidly to  $\sim 3\text{\AA}$ , and stays there for a while. The conformation eventually relaxes into the final state, dRMSD  $\sim 1.5\text{\AA}$ . This final state is actually the near-rigor state, judging from its average structure; in fact, the dRMSD of the average structure is  $\sim 1\text{\AA}$ . In short, the myosin motor domain in the pre-power stroke conformation relaxes at first into the intermediate state and then to the near-rigor conformation.

We introduced an index to characterize the state of the nucleotide binding,  $Q_{\text{nucl}}(\Gamma)$ ; we count how many of the nucleotide contacts that is formed in structure 2 (the pre-power stroke) remain in a given conformation,  $\Gamma$ . Then,  $Q_{\text{nucl}}(\Gamma)$  is defined as this number divided by the number of nucleotide contacts in structure 2.  $Q_{\text{nucl}} \sim 1$  when a nucleotide is bound, and  $Q_{\text{nucl}} = 0$  if the nucleotide-binding site is empty. The time courses of  $Q_{\text{nucl}}$  are also shown in Fig. 3. The structural relaxation occurs after or, at the earliest, at the same time as the nucleotide dissociation. Furthermore, the relaxation tends to synchronize with the dissociation as  $k_{p-n}$  increases. To clarify the  $k_{p-n}$  dependency of the synchronization, we plotted the histograms of  $\tau_d$  and of  $\Delta\tau = \tau_d - \tau_r$  from 200 independent runs for each value of  $k_{p-n}$ , where  $\tau_d$  is the number of steps taken before the nucleotide dissociates,  $\tau_r$  is the number of steps taken before the conformation relaxes to the near-rigor state, and  $\Delta\tau$  is the delay in the relaxation after the dissociation takes place (Fig. 4).

For small  $k_{p-n}$ , both the histograms of both  $\tau_d$  and of  $\Delta\tau$  show exponential decay; thus, the nucleotide dissociation and the relaxation of the myosin conformation are considered to be decoupled. For larger  $k_{p-n}$ , on the other hand, the histogram of  $\tau_d$  cannot be fitted to an exponential decay. In addition, the average of  $\tau_d$  is shifted to the right and the delays,  $\Delta\tau$  become shorter; in other words, the nucleotide is unbound later and the conformational relaxation tends to occur immediately after the nucleotide dissociation. For  $k_{p-n} = 0.7$ , dissociation and relaxation occur nearly simultaneously in over 60% of 200 trajectories. Note that apparent “ $\Delta\tau < 0$  cases” are caused simply from the numerical ambiguity of  $\tau_d$  and  $\tau_r$  and actually correspond to coincidental dissociation-relaxation.

The largest difference between the intermediate state and

the initial (pre-power stroke) conformation is the position of the converter domain with respect to the other subdomains; the relative positions among other subdomains (for example, the N terminal and the 50-kDa subdomain) are similar to those in the pre-power stroke conformation. The average dRMSD of the intermediate state varies slightly with the parameter  $k_{p-n}$  (Fig. 5), reflecting little difference in the position of the converter relative to the other subdomains.

Some of the native contacts of structure 1 are not formed until the conformation finally relaxes to the near-rigor state. Figure 6 shows the residues included in these contacts. They are concentrated at the boundary between the N terminal and the 50-kDa subdomain, that is, the region around the nucleotide-binding site. Thus, the final relaxation process consists of a rearrangement of the N terminal subdomain against the other part.

As already mentioned, the myosin motor domain relaxes to the near-rigor conformation only after the dissociation of the nucleotide and not before. Thus, it seems that the nucleotide must be unbound for the final relaxation to occur. This observation leads to a speculation that the nucleotide blocks the deformation of myosin around the nucleotide-binding site by its volume. To investigate the case of when the nucleotide cannot dissociate, we attempted a nucleotide-free and constrained simulation. In this simulation, instead of treating the nucleotide molecule explicitly, we connected the residues that would contact with the nucleotide by virtual bonds, to force the nucleotide-binding site to keep the pre-power stroke form. Figure 5 shows the time courses obtained by the simulations. We find that the conformation remains at the intermediate state and that the relaxation toward the near-rigor state is not completed.

## Discussion

The relaxation simulation using coarse-grained myosin and the nucleotide have shown that the myosin motor domain does not relax to the near-rigor conformation before the nucleotide dissociates. Ishijima *et al.* [22] showed by simultaneous observation of ADP release and mechanical events that force is generated at the same time as or several hundreds of milliseconds after the dissociation of ADP. Our results are consistent with their experimental findings if force generation is preceded by structural relaxation. Moreover, the results from the simulations in which the conformation of the nucleotide-binding site is constrained also indicate that the relaxation is indeed prevented if the nucleotide cannot dissociate.

Based on these observations, we now suggest that the primary role of the nucleotide in the “power stroke” process is to suppress relaxation through blocking deformation around the nucleotide-binding site by its volume. In this scenario, hydrolysis is required to alter the affinity of the nucleotide to the binding site. In particular, our simulations have shown that the structural relaxation is synchronous with nucleotide dissociation when the nucleotide is tightly bound to the myosin head. In other words, the nucleotide dissociates cooperatively with the motion of the subdomain. This strong coupling of deformation and dissociation seems to be relevant to the function of the “strain sensor,” in which nucleotide dissociation is controlled by the strain induced by an external force. The correlation depends on the binding strength,  $k_{p-n}$ ; the relaxation is only loosely coupled with the dissociation for weak bind-

ing conditions. The origin of a large kinetic diversity among myosins [23, 24] may be attributed to this binding strength dependence.

The intermediate state observed in the relaxation process should also be discussed. Although several intermediate states have been revealed by kinetic experiments[23], their structural aspects, except for ADP·P<sub>i</sub> state, are little known. Shih *et al.* [25] reported, from their FRET study, that there are two “pre-power stroke” conformations; while one conformation corresponds to the crystal structure of the complex with the ADP·P<sub>i</sub> analog, the other conformation has not yet been observed using crystallography. We found that the average structure of the intermediate state observed in the present study is consistent with the latter conformation.

Our dual G $\bar{o}$  model is effective in studying myosin conformational changes. Recently, a similar approach was proposed for a Monte Carlo simulation of a lattice protein, in which a double-square-well potential for native-contact pairs was introduced[26]. This type of model, in which two conformations are embedded in an energy potential function, will be useful in understanding the dynamics of protein conformational change.

## Models and Methods

Our dual G $\bar{o}$ -model is a variant of the C $_{\alpha}$  G $\bar{o}$ -like model [18, 19]. A protein chain is formed, consisting of spherical beads that represent C $_{\alpha}$  atoms of amino acid residues connected by virtual bonds. In conventional G $\bar{o}$ -like models, only amino acid pairs that contact in the native conformation are assigned an effective energy. In the dual G $\bar{o}$ -model, on the other hand, the effective energy function takes two reference structures, structure 1 and structure 2. A nucleotide molecule is also expressed as a chain of connected beads.

The total energy of the system,  $U_{\text{tot}}$  consists of three terms;

$$U_{\text{tot}} = U_p + U_n + U_{p-n}, \quad [2]$$

where  $U_p$  is the intraprotein interaction,  $U_n$  is the intranucleotide interaction, and  $U_{p-n}$  is the interaction between protein and nucleotide.

The effective protein energy  $U_p$  at a conformation  $\Gamma$  is given as,

$$U_p(\Gamma, \Gamma^{(1)}, \Gamma^{(2)}) = U^b + U^\theta + U^\phi + U^{\text{nc}} + U^{\text{nnc}}. \quad [3]$$

where  $\Gamma^{(1)}$  and  $\Gamma^{(2)}$  stand for the conformations of the two reference structures. The terms in Eq. 3 are defined as follows:

$$U^z = \sum_i \min\{V_z^{(1)}(z_i), V_z^{(2)}(z_i)\}, \quad [4]$$

$$U^{\text{nc}} = \sum_{j < i-3}^{\text{native contact}} \min\{V_{\text{nc}}^{(1)}(\mathbf{r}_{ij}), C_{12} V_{\text{nc}}^{(2)}(\mathbf{r}_{ij})\}, \quad [5]$$

$$U^{\text{nnc}} = \sum_{j < i-3}^{\text{non-native contact}} V_{ij}^{\text{nnc}}(\mathbf{r}_{ij}), \quad [6]$$

where  $z$  stands for  $b$ ,  $\theta$  or  $\phi$ , and (1) and (2) again indicate the reference conformations. The vector  $\mathbf{r}_{ij} = \mathbf{r}_i - \mathbf{r}_j$  is the distance between the  $i$ th and  $j$ th C $_{\alpha}$ , where  $\mathbf{r}_i$  is the position of the  $i$ th C $_{\alpha}$ .  $b_i = |\mathbf{b}_i| = |\mathbf{r}_{i+1}|$  is the virtual bond length

between two adjacent  $C_\alpha$ .  $\theta_i$  is the angle between two adjacent virtual bonds, where  $\cos\theta_i = \mathbf{b}_{i-1} \cdot \mathbf{b}_i / b_{i-1}b_i$ , and  $\phi_i$  is the  $i$ th dihedral angle around  $\mathbf{b}_i$ . The first three terms of Eq. 3 provide local interactions, while the last two terms are interactions between non-local pairs that are distant along the chain.

For potential functions,  $V_Z^{(\alpha)}$ ,  $V_{\text{nc}}^{(\alpha)}$ , and  $V_{\text{nnc}}^{(\alpha)}$ , we use the same functions as Clementi *et al.* [18]:

$$V_{\text{b}}^{(\alpha)}(b_i) = k_{\text{b}}(b_i - b_i^{(\alpha)})^2, \quad [7]$$

$$V_{\theta}^{(\alpha)}(\theta_i) = k_{\theta}(\theta_i - \theta_i^{(\alpha)})^2, \quad [8]$$

$$V_{\phi}^{(\alpha)}(\phi_i) = k_{\phi} \left[ \left( 1 - \cos(\phi_i - \phi_i^{(\alpha)}) \right) + \frac{1}{2} \left( 1 - \cos 3(\phi_i - \phi_i^{(\alpha)}) \right) \right], \quad [9]$$

$$V_{\text{nc}}^{(\alpha)}(\mathbf{r}_{ij}) = k_{\text{nc}} \left[ 5 \left( \frac{r_{ij}^{(\alpha)}}{r_{ij}} \right)^{12} - 6 \left( \frac{r_{ij}^{(\alpha)}}{r_{ij}} \right)^{10} \right], \quad [10]$$

$$V_{ij}^{\text{nnc}}(\mathbf{r}_{ij}) = k_{\text{nnc}} \left( \frac{C}{r_{ij}} \right)^{12}, \quad [11]$$

where the superscript  $\alpha$  is 1 or 2 and represents the appropriate reference structure. Parameters with superscript 1 or 2 are constants taken from the corresponding values in structure 1 or 2, respectively. For the local interaction terms (bond length, bond angle, and dihedral angle), the potential energy for each set of beads takes the smaller of  $V^{(1)}$  and  $V^{(2)}$ . For example, the length of the  $i$ th bond is  $b_i^{(1)}$  in structure 1 and is  $b_i^{(2)}$  in structure 2; therefore, the potential energy for this bond is  $k_{\text{b}} \min\{(b_i - b_i^{(1)})^2, (b_i - b_i^{(2)})^2\}$ . We specify (define) that the  $i$ th and  $j$ th amino acids are in the “native contact pair” of structure 1 (or structure 2) if one of the non-hydrogen atoms in the  $j$ th amino acid is within 6.5 Å of one of the non-hydrogen atoms in the  $i$ th amino acid at the structure 1 (or structure 2). The interaction potential for each native-contact pair,  $ij$ , takes the smaller of  $V_{\text{nc}}^{(1)}(\mathbf{r}_{ij})$  and  $C_{12}V_{\text{nc}}^{(2)}(\mathbf{r}_{ij})$ .  $C_{12}$  is the ratio of the potential depth of structure 2 to that of structure 1 (Fig.7). Here, since we intend to perform simulations of the structural change from structure 2 to structure 1, that is, we want to structure 1 as the final stable structure, we assign a value smaller than unity to  $C_{12}$  ( $C_{12} = 0.8$ ). If a residue pair  $ij$  is a native-contact pair in structure 1 but not in structure 2 (or vice versa), the interaction potential between the  $i$ th and  $j$ th residues is a Lennard-Jones potential,  $V_{\text{nc}}^{(1(\text{or}2))}(\mathbf{r}_{ij})$ , with a single minimum. Other relevant parameters are  $k_{\text{b}} = 100.0$ ,  $k_{\theta} = 20.0$ ,  $k_{\phi} = 1.0$ ,  $k_{\text{nc}} = k_{\text{nnc}} = 0.25$ , and  $C = 4.0$ . The cut-off length for calculating  $V_{\text{nc}}^{(\alpha)}$  is taken to be  $2r_{ij}^{(\alpha)}$ .

To understand the mechanism of the actomyosin motor, it is desirable to study the conformational change to the rigor state. However, currently no X-ray crystal structure is currently available for a true rigor complex with actin; therefore, we studied the structural relaxation from the pre-power stroke state to the near-rigor state. Structures 1 and 2 thus correspond to the near-rigor and pre-power stroke structures, respectively. We used 1Q5G [20], which is the nucleotide free structure of *Dictyostelium discoideum* myosin II, as the near-rigor state. Although a few nucleotide-free structures of

myosin II have been determined, only 1Q5G is regarded to be the near-rigor state, because both switch I and switch II are in the open position. We chose 1VOM [21] for the pre-power stroke structure. It includes an ADP·P<sub>i</sub> analog (ADP·VO<sub>4</sub>) in the nucleotide binding site. While 1Q5G consists of residues 2-765 without a gap region, 1VOM includes only residues 2-747 and has gap regions where the structure has not been determined by X-ray crystallography. Therefore we used the structures of residues 2-747 for simulations. Potential functions of the near-rigor conformation are assigned for local interactions in the gap region.

The nucleotide molecule (ADP·VO<sub>4</sub> in 1VOM) is also included in the simulation as a coarse-grained chain (Fig. 2). The coarse-grained ADP·VO<sub>4</sub> is represented as a short linear chain of five beads, corresponding to a purine base, a sugar (ribose), two phosphates, and VO<sub>4</sub> (a phosphate analog). The intranucleotide interaction is defined as

$$U_{\text{n}} = \sum_k k_{\text{b}} (|\mathbf{r}_{k+1} - \mathbf{r}_k| - |\mathbf{r}_{k+1}^{(2)} - \mathbf{r}_k^{(2)}|)^2 + \sum_k k_{\text{b}} (|\mathbf{r}_{k+2} - \mathbf{r}_k| - |\mathbf{r}_{k+2}^{(2)} - \mathbf{r}_k^{(2)}|)^2. \quad [12]$$

The interaction potential between the protein and the nucleotide is similar to that between the non-local residues in the protein. Here, we assume that only structure 2 includes the nucleotide: therefore, the potential function has only a single well (the standard Lennard-Jones potential). We specify that the  $i$ th residue of the protein and the  $k$ th bead in the nucleotide chain should be in “native-contact” in the pre-power stroke conformation when one of the non-hydrogen atoms in the  $k$ th bead (base or sugar of P<sub>i</sub>) is within 4.5 Å of one of the non-hydrogen atoms in the  $i$ th amino acid. The residues that form native-contacts with the nucleotide are called nucleotide-contact residues:

$$U_{\text{p-n}}(\mathbf{r}_{ik}) = \sum_{i,k}^{\text{native contact}} k_{\text{p-n}} \left[ 5 \left( \frac{r_{ik}^{(2)}}{r_{ik}} \right)^{12} - 6 \left( \frac{r_{ik}^{(2)}}{r_{ik}} \right)^{10} \right] + \sum_{j < i-3}^{\text{non-native contact}} k_{\text{nnc}} \left( \frac{C}{r_{ik}} \right)^{12}, \quad [13]$$

where  $i$  stands for the  $i$ th residue and  $k$  stands for the  $k$ th bead in the nucleotide chain.

The dynamics of the proteins are simulated using the Langevin equation at a constant temperature  $T$ ,

$$m_i \dot{\mathbf{v}}_i = \mathbf{F}_i - \gamma \mathbf{v}_i + \xi_i \quad [14]$$

where  $\mathbf{v}$  is the velocity of the  $i$ th bead and a dot represents the derivative with respect to time  $t$  (thus,  $\mathbf{v}_i = \dot{\mathbf{r}}_i$ ), and  $\mathbf{F}_i$  and  $\xi_i$  are systematic and random forces acting on the  $i$ th bead, respectively. The systematic force  $\mathbf{F}_i$  is derived from the effective potential energy  $U$  and can be defined as  $\mathbf{F}_i = -\partial U / \partial \mathbf{r}_i$ .  $\xi_i$  is a Gaussian white random force, which satisfies  $\langle \xi_i \rangle = 0$  and  $\langle \xi_i(t) \xi_j(t') \rangle = 2\gamma T \delta_{ij} \delta(t-t') \mathbf{1}$ , where the bracket denotes the ensemble average and  $\mathbf{1}$  is a  $3 \times 3$  unit matrix. We used an algorithm by Honeycutt and Thirumalai [27] for a numerical integration of the Langevin equation, We used  $\gamma = 0.25$ ,  $m_i = 1.0$ , and the finite time step  $\Delta t = 0.02$ .

For a given protein conformation,  $\Gamma$ , we note that the native contact of structure 1 (or 2) between  $i$  and  $j$  is formed

if the  $C_\alpha$  distance  $r_{ij} = |\mathbf{r}_{ij}|$  satisfies  $0.8r_{ij}^{(1)} < r_{ij} < 1.2r_{ij}^{(1)}$  ( $0.8r_{ij}^{(2)} < r_{ij} < 1.2r_{ij}^{(2)}$ ).

Simulations were started from the pre-power stroke structure. The initial positions of residues in the gap regions of IVOM were set randomly under the condition that the bond length was 3.8 Å. The initial velocities of each bead was given to satisfy the Maxwell distribution. The temperature was set lower than the folding temperature for structure 1.

We also ran a nucleotide-free and constrained simulation, in which the nucleotide was not explicitly included but the relative positions of the nucleotide-contact residues were constrained by virtual bonds in all-to-all correspondence to keep the pre-power stroke form. The natural length of the virtual

bonds  $i$ - $j$ ,  $r_{ij}^{(2)}$ , is the  $C_\alpha$  distance between the  $i$ th and  $j$ th residues in the pre-power stroke conformation (structure 2). The total effective potential energy was  $U_P + U_{\text{con}}$ , and

$$U_{\text{con}} = \sum_{j < i}^{\text{nucl.-contact}} k_{\text{con}} (r_{ij} - r_{ij}^{(2)})^2, \quad [15]$$

where  $k_{\text{con}} = 1.0$ .

We thank Shoji Takada and Toshio Yanagida for many helpful suggestions. This work was supported by IT-program of the Ministry of Education, Culture, Sports, Science and Technology, and Grant-in-Aid for Scientific Research (C) (17540383) from the Japan Society for the Promotion of Science.

1. Geeves, M. A & Holmes, K. C. (1999) *Ann. Rev. Biochem.* **68**, 687–728.
2. Kitamura, K, Tokunaga, M, Esaki, S, Iwane, A. H, & Yanagida, T. (2005) *BIOPHYSICS* **1**, 1–19.
3. Spudich, J. A. (2001) *Nat. Rev. Mol. Cell Biol.* **2**, 387–392.
4. Yanagida, T, Arata, T, & Oosawa, F. (1985) *Nature* **316**, 366–369.
5. Vale, R. D & Oosawa, F. (1990) *Advances in biophysics.* **26**, 97–134.
6. Julicher, F, Ajdari, A, & Prost, J. (1997) *Rev. Mod. Phys.* **69**, 1269–1281.
7. Reimann, P. (2002) *Physics Reports* **361**, 57–265.
8. Veigel, C, Molloy, J. E, Schmitz, S, & Kendrick-Jones, J. (2003) *Nat. Cell. Biol.* **5**, 980–986.
9. Veigel, C, Schmitz, S, Wang, F, & Sellers, J. R. (2005) *Nat. Cell. Biol.* **7**, 861–869.
10. Altman, D, Sweeney, H. L, & Spudich, J. A. (2004) *Cell* **116**, 737–749.
11. Huxley, A. F. (1957) *Progress in Biophysics and Biophysical Chemistry.* **7**, 255–318.
12. Cui, Q, Li, G, Ma, J, & Karplus, M. (2004) *J. Mol. Biol.* **340**, 345–372.
13. Ikeguchi, M, Ueno, J, Sato, M, & Kidera, A. (2005) *Phys. Rev. Lett.* **94**, 078102–4.
14. Zheng, W & Doniach, S. (2003) *Proc. Natl. Acad. Sci. USA* **100**, 13253–13258.
15. Koga, N & Takada, S. (2006) *Proc. Natl. Acad. Sci. USA* **103**, 5367–5372.
16. Go, N. (1983) *Annu. Rev. Biophys. Bioeng.* **12**, 183–210.
17. Onuchic, J. N, Luthey-Schulten, Z, & Wolynes, P. G. (1997) *Annu. Rev. Phys. Chem.* **48**, 545–600.
18. Clementi, C, Nymeyer, H, & Onuchic, J. N. (2000) *J. Mol. Biol.* **298**, 937–953.
19. Koga, N & Takada, S. (2001) *J. Mol. Biol.* **313**, 171–180.
20. Reubold, T. F, Eschenburg, S, Becker, A, Kull, F. J, & Manstein, D. J. (2003) *Nat. Struct. Biol.* **10**, 826–830.
21. Smith, C. A & Rayment, I. (1996) *Biochemistry* **35**, 5404–5417.
22. Ishijima, A, Kojima, H, Funatsu, T, Tokunaga, M, Higuchi, H, Tanaka, H, & Yanagida, T. (1998) *Cell* **92**, 161–171.
23. Cruz, E. M. D. L & Ostap, E. M. (2004) *Current Opinion in Cell Biology* **16**, 61–67.
24. Sellers, J. R. (2000) *Biochem. Biophys. Acta* **1496**, 3–22.
25. Shih, W. M, Gryczynski, Z, Lakowicz, J. R, & Spudich, J. A. (2000) *Cell* **102**, 683–694.
26. Zuckerman, D. (2004) *J. Phys. Chem. B* **108**, 5127–5137.
27. Honeycutt, J. D & Thirumalai, D. (1992) *Biopolymers* **32**, 695–709.

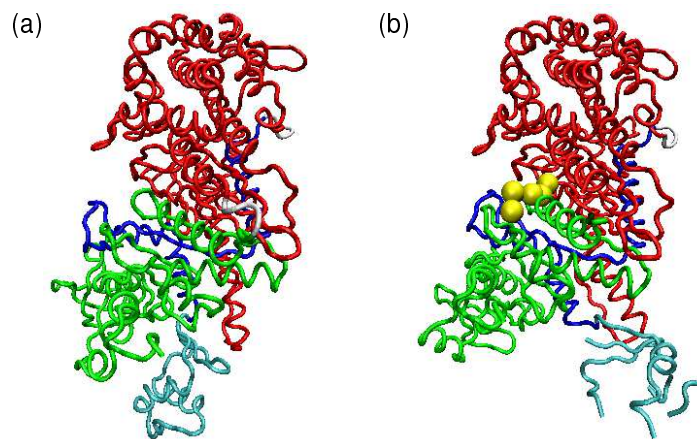


**Fig. 1.** We chose (a) near-rigor structure, 1Q5G, and (b) pre-power stroke structure, 1VOM for structure 1 and 2, respectively. 1VOM contains the ADP·P<sub>i</sub> analog, ADP·VO<sub>4</sub> (yellow). Also shown are the N-terminal (green), 50 kDa subdomain (red) and the converter (cyan) included in C-terminal subdomain (blue) that is connected to the lever arm.

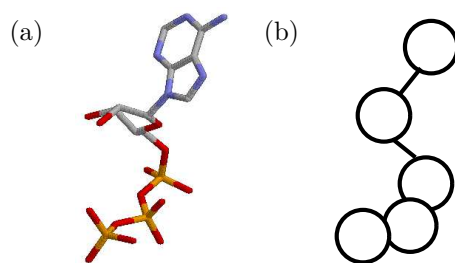


**Fig. 2.** (a) ATP and (b) coarse-grained ATP.

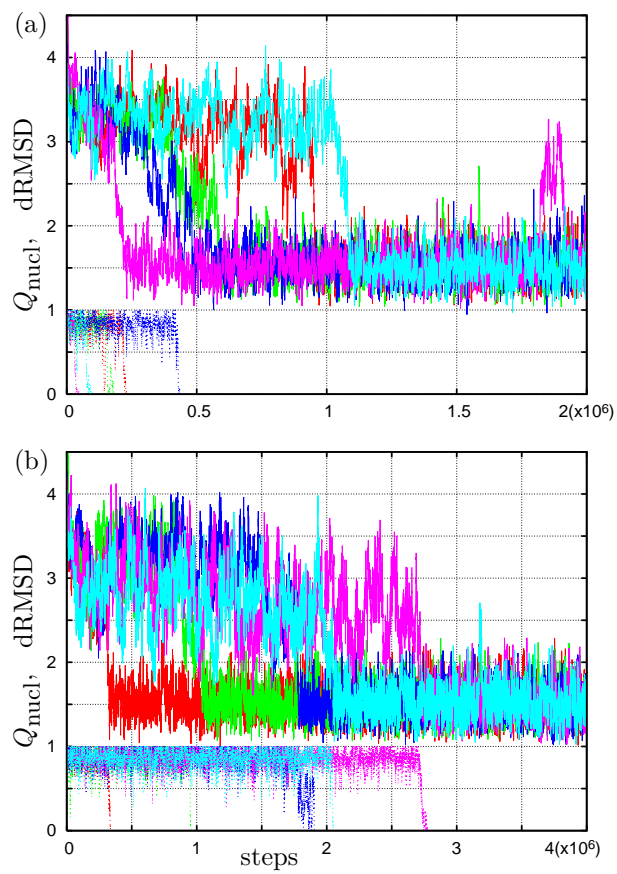


**Fig. 3.** Relaxation time courses of dRMSD (from 1Q5G) (solid line) and  $Q_{\text{nucl.}}$  (dotted line) for five trajectories are shown. Different colors distinguish different runs. (a)  $k_{\text{p-n}} = 0.6$ , (b)  $k_{\text{p-n}} = 0.7$

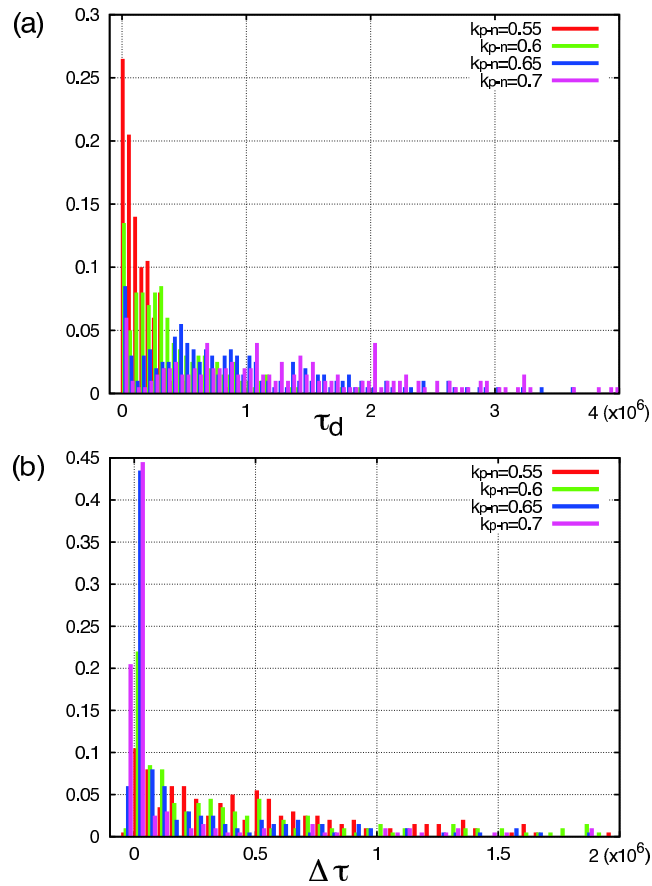


**Fig. 4.** Histogram of (a) the number of steps before dissociation and (b) the delay of the relaxation after the dissociation from 200 independent runs for each  $k_{p-n}$ .

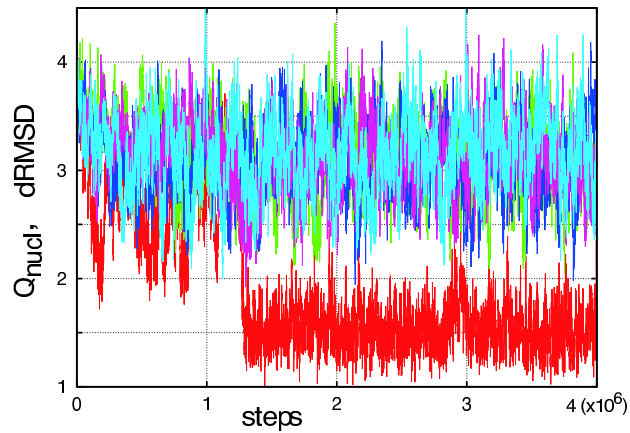


**Fig. 5.** Time sequence of dRMSD. The red line is the trajectory of the no-constraint simulation, and the other lines are trajectories of simulations in which nucleotide-binding site are constrained.





**Fig. 6.** Residues included in the contacts that are formed at the final relaxation to the near-rigor.

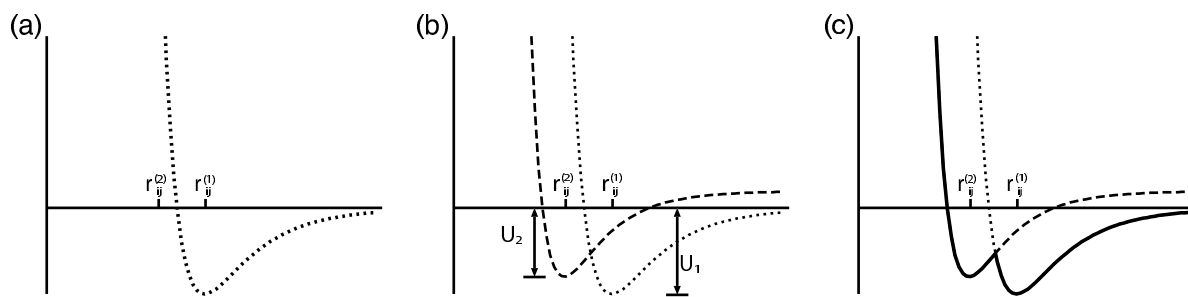


**Fig. 7.** Gō-potential: The magenta line is dual Gō-potential energy profile for the  $ij$  pair.  $C_{12} = U_2/U_1$ .